

Proton Tolerance of Fourth-Generation 350 GHz UHV/CVD SiGe HBTs

Akil K. Sutton, *Student Member, IEEE*, Becca M. Haugerud, *Student Member, IEEE*, Yuan Lu, *Student Member, IEEE*, Wei-Min Lance Kuo, *Student Member, IEEE*, John D. Cressler, *Fellow, IEEE*, Paul W. Marshall, *Member, IEEE*, Robert A. Reed, *Member, IEEE*, Jae-Sung Rieh, *Member, IEEE*, Greg Freeman, *Senior Member, IEEE*, and David Ahlgren

Abstract—We report, for the first time, the impact of proton irradiation on 4th-generation SiGe HBTs having a record peak unity gain cutoff frequency of 350 GHz. The implications of aggressive vertical scaling on the observed proton tolerance is investigated through comparisons of the pre- and post-radiation *ac* and *dc* figures-of-merit to observed results from prior SiGe HBT technology nodes irradiated under identical conditions. In Additional, transistors of varying breakdown voltage are used to probe the differences in proton tolerance as a function of collector doping. Our findings indicate that SiGe HBTs continue to exhibit impressive total dose tolerance, even at unprecedented levels of vertical profile scaling and frequency response. Negligible total dose degradation in β (0.3%), f_T and f_{max} (6%) are observed in the circuit bias regime, suggesting that SiGe HBT BiCMOS technology is potentially a formidable contender for high-performance space-borne applications.

I. MOTIVATION

Silicon-Germanium Heterjunction Bipolar Transistors (SiGe HBTs) continue to emerge as a viable technology option for terrestrial monolithic RF, microwave, and even millimeter ICs used in broadband communications systems. SiGe HBTs exhibit performance characteristics as good as, or better than III-V technologies, while leveraging seamless integration with traditional low cost, high yield Si-based CMOS fabrication [1]. This synergy enables the technology to be incorporated into SiGe BiCMOS system-on-a-chip (SoC) integration schemes that can be tailored to produce "commercial-off-the-shelf" (COTS) modules for communications systems.

The 4th-generation SiGe HBTs under investigation here were fabricated at IBM Microelectronics (IBM 9T), and achieve a remarkable peak cutoff frequency (f_T) of 350 GHz, a record for any Si-based transistor. This unprecedented level of frequency response represents a 67% increase over the previous SiGe HBT performance record, and was fabricated in 120 nm 100% Si-compatible technology, as detailed in [2]. Process windows currently enable the realization of peak f_T and f_{max} both above 300GHz through careful optimization, as recently reported in [3], but the present work features a non-optimized f_{max} of 170GHz, as illustrated in Figure 1. The associated BV_{CEO} and BV_{CBO} are 1.4 V and 5.0 V, respectively, yielding an $f_T BV_{CEO}$ product well

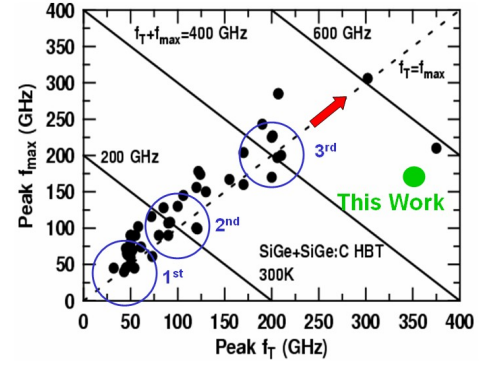


Fig. 1. Comparison of SiGe HBT technology nodes in the f_T - f_{max} space.

above the so-called 200 GHz V "Johnson limit" [4].

A discussion of the scaling methodologies employed in the first two distinct technology generations (IBM 5HP and 7HP), and the resultant effects on the observed proton tolerance, has been investigated in [5], and for brevity are not revisited here. In the 3rd-generation SiGe technology (IBM 8HP), an improvement in f_T to 200 GHz was realized only through fundamental changes in the physical structure of the transistor. Specifically, a reduced thermal cycle "raised extrinsic base" structure was implemented using conventional deep and shallow trench isolation (STI), and an *in situ* doped polysilicon emitter. The SiGe base region featured an unconditionally stable, 25% peak Ge, C-doped profile deposited using UHV/CVD epitaxial growth techniques as described in [6]. This new structure, depicted in Figure 2, raises serious concerns regarding the spatial distribution of radiation induced trap centers previously determined to be primarily located near the STI edges alongside the emitter-base (EB) spacer [7].

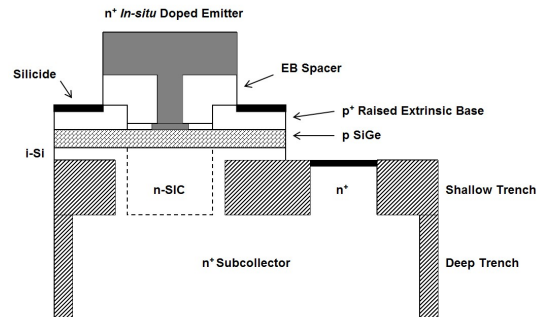


Fig. 2. Representative cross-section of a 4th-generation SiGe HBT.

This work was supported by DTRA under the Radiation Tolerant Microelectronics Program, NASA-GSFC under the Electronics Radiation Characterization Program, IBM, and the Georgia Electronic Design Center at Georgia Tech.

A.K. Sutton, J.D. Cressler B.M. Haugerud, W.-M.L. Kuo and Y. Lu are with the School of Electrical and Computer Engineering, 85 Fifth Street, N.W., Georgia Institute of Technology, Atlanta, GA 30308, USA.

Tel: (404) 894-5161 / Fax: (404) 894-4641 / E-mail: asutton@ece.gatech.edu

P.W. Marshall is a consultant to NASA-GSFC.

R.A. Reed is with NASA-GSFC, Greenbelt, MD 20771 USA.

J.-S. Rieh, G. Freeman, and D. Ahlgren are with IBM Microelectronics, Hopewell Junction, NY 12533 USA.

Investigations into the proton tolerance of this 3rd-generation structure concluded that total dose tolerance had been maintained [8], however, as a result of pre-existing generation-recombination (GR) trap centers prior to irradiation there was some uncertainty as to the degree of masking of any additional radiation induced traps. In the case of the new 4th-generation technology (same representative cross-section as for the 3rd-generation technology), performance enhancements were realized primarily through careful profile optimization and aggressive vertical scaling of the base and collector regions, resulting in a record emitter-to-collector transit time (τ_{EC}) of 0.45 psec[2]. The key fabrication parameters that were adjusted to realize such performance include the base width (W_b), germanium content, and dopant profiles, as highlighted in the representative SIMS doping profile of a 1st-generation device illustrated in Figure 3.

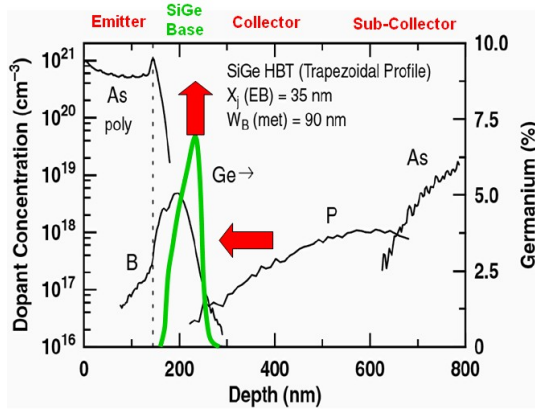


Fig. 3. Representative SIMS profile of a 1st-generation technology.

The impact of combining this unprecedented level of vertical profile scaling on the proton radiation response is investigated for the first time using these 350 GHz SiGe HBTs. A comprehensive picture of the variation in total dose tolerance across multiple SiGe technology platforms is presented by drawing quantitative comparisons between 1st (IBM 5HP), 2nd (IBM 7HP), 3rd (IBM 8T), and now 4th (IBM 9T) generation SiGe technology nodes.

II. EXPERIMENT

The 4th-generation 350 GHz SiGe HBTs investigated here feature an emitter area (A_E) of $0.12 \times 2.5 \mu\text{m}^2$, and were compared to $0.50 \mu\text{m}$ 50 GHz (IBM 5HP), $0.20 \mu\text{m}$ 120 GHz (IBM 7HP), and $0.12 \mu\text{m}$ 200 GHz (IBM 8T) technology nodes measured under identical conditions in order to facilitate unambiguous comparisons. Multiple breakdown voltage transistors were fabricated on-wafer using different collector implantation (N_C), and were used to assess the impact of the collector doping profile on measured proton response.

The samples were irradiated with 63.3 MeV protons at the Crocker Nuclear Laboratory at the University of California at Davis. The dosimetry measurements used a five-foil secondary emission monitor calibrated against a Faraday cup. The radiation source (Ta scattering foils) located several meters upstream of the target establish a beam spatial uniformity of about 15% over a 2.0 cm radius circular area. Beam currents from about 20 nA to 100 nA allow testing with proton fluxes from 1×10^9 to

1×10^{12} proton/cm²sec. The dosimetry system has been previously described[9] [10], and is accurate to about 10%. At proton fluences of 1×10^{12} p/cm² and 5×10^{13} p/cm², the measured equivalent total ionizing dose was approximately 135 and 6,759 krad(Si), respectively. The SiGe HBTs were irradiated with all terminals grounded for the *dc* measurements and with all terminals floating for the *ac* measurements at proton fluences ranging from 1.0×10^{12} p/cm² to 5.0×10^{13} p/cm². The *ac* measurement samples, which were irradiated at 7.0×10^{12} p/cm² and 5.0×10^{13} p/cm², were measured and then subsequently re-irradiated at the same fluence levels. Thus, when re-characterized, the *ac* samples were irradiated to maximum net proton fluences of 1.4×10^{13} p/cm² and 1.0×10^{14} p/cm². We have previously shown that SiGe HBTs are not sensitive to applied bias during irradiation [1]. Wirebonding of *ac* test structures is not compatible with robust broadband measurements, and hence on-wafer probing of S-parameters (with terminals floating) was used to characterize the high-frequency device performance. The post-irradiated samples were characterized at room temperature with an Agilent 4155 Semiconductor Parameter Analyzer (*dc*) and an Agilent 8510C Vector Network Analyzer (*ac*) using the deembedding techniques discussed in [11].

III. *dc* RESULTS

The post-irradiation forward-mode Gummel characteristics on a low-breakdown transistor are shown in Figure 4 and clearly indicates a base current density (J_B) that is a monotonically increasing function of proton fluence. This classical signa-

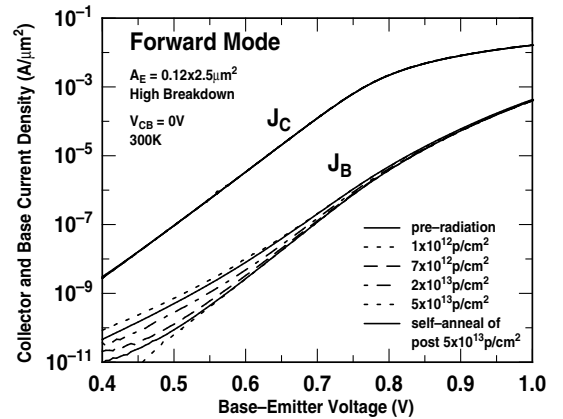


Fig. 4. Forward-mode Gummel characteristics (4th-generation).

ture of radiation-induced damage in SiGe HBTs is attributed to radiation-induced GR trap centers, physically located near the emitter-base spacer oxide and shallow-trench isolation (STI) edges [7]. Measurements performed at room temperature, approximately 6 weeks after the exposure yielded a slight decrease in J_B , indicative of a "self-annealing" mechanism. Similar results obtained for the inverse-mode Gummel characteristics (emitter and collector terminals swapped) are illustrated in Figure 5. At the low fluence of 1×10^{12} p/cm² (135krad(Si)), there is a slight reduction in both the forward- and inverse-mode J_B at very low base-emitter voltages, presumably the manifestation of an underlying radiation-induced annealing of pre-existing G/R traps.

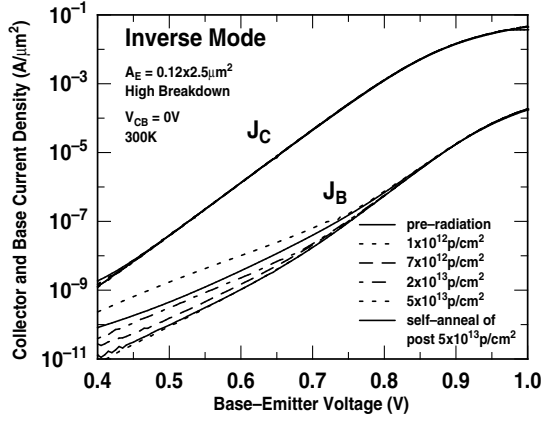


Fig. 5. Inverse-mode Gummel characteristics (4th-generation).

The forward-mode dc current gain (β) is depicted in Figure 6, and shows a consistent degradation with increasing proton fluence, as expected. There is over 40% decrease in β_{peak} coincident with a shift in the occurrence of β_{peak} to higher J_C . More importantly, however, there is practically no change (less than 0.3% decrease) in β at peak f_T , which is the figure-of-merit of primary concern for most circuit designers.

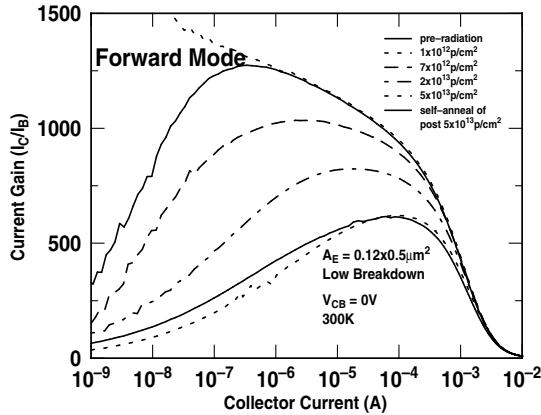


Fig. 6. Forward-mode current gain (4th-generation).

Three dc figures-of-merit were used to compare the proton tolerance across multiple SiGe HBT technology generations: the β_{peak} degradation, and the forward-mode and inverse-mode I_B degradation (sampled at $V_{BE} = 0.6V$). Our previous work attributed the increased radiation-induced I_B leakage in 2nd- that found in 1st-generation SiGe HBTs to the increased electric field in the emitter-base (EB) junction at the device periphery, and associated with the higher local doping associated with vertical and lateral scaling [5]. Figures 7 and 8 demonstrates that there are substantial improvements in both the forward- and inverse-mode post-radiation I_B degradation respectively (for both 3rd-, and 4th-generation). Finally, an analysis of β_{peak} degradation reveals that the 4th- generation devices, with their improved performance, exhibit a degradation similar to that of the 1st-generation device (and slightly better degradation for the high-breakdown device).

This improved radiation tolerance can be explained by the fact that for both the 3rd-, and 4th- generation devices the "raised

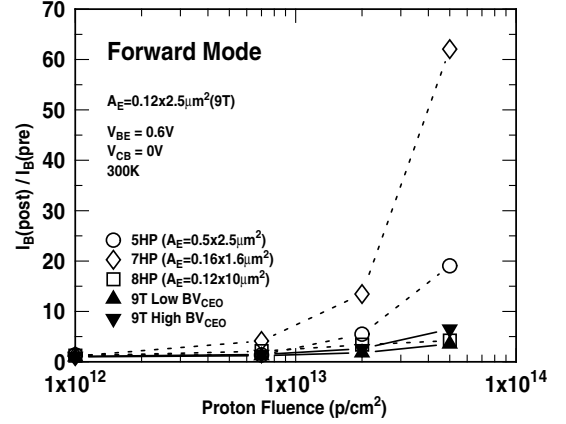


Fig. 7. Forward-mode I_B degradation (1st-, 2nd-, 3rd- and 4th-generation).

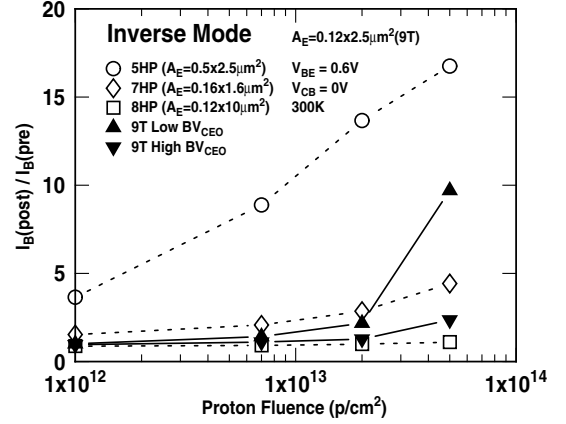


Fig. 8. Inverse-mode I_B degradation (1st-, 2nd-, 3rd- and 4th-generation).

extrinsic base" configuration results in EB(*forward - mode*) and CB(*inverse - mode*) junctions that are physically further removed from the STI edges. Therefore, the effective trap density near the both junctions is such that there is less carrier recombination and hence ΔI_B is reduced. It should be emphasized that these improvements are achieved solely through the migration to the new raised extrinsic base structure and also compare well with the non-ideal 3rd- generation devices investigated in [8].

IV. BREAKDOWN CONSIDERATIONS

A closer look at the inverse-mode I_B degradation of the 4th-generation SiGe HBT shown in Figure 8 indicates that the low-breakdown transistors (with their higher collector doping, N_C) are slightly more susceptible to proton induced damage at the CB junction than those with a higher-breakdown. In the low-breakdown device N_C is increased to delay the onset of high injection heterojunction barrier effects (HBE) and Kirk effect [12]. Typically, this yields an increased collector-base charge capacitance (C_{CB}) and avalanche multiplication ($M - 1$) that results in a reduced f_{max} and BV_{CEO} respectively [1]. However, careful collector profile optimization can be employed to simultaneously realize improvement in both f_T and BV_{CEO} [13], [14]. In the case of the devices under study, an increased N_C translates into a CB junction now pushed physically closer to the STI edge where the radiation induced G/R trap density is high. The extrin-

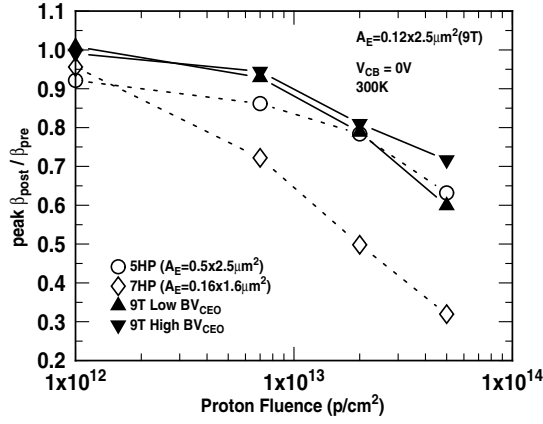


Fig. 9. β_{peak} degradation for for (1st-, 2nd-, 3rd- and 4th-generation).

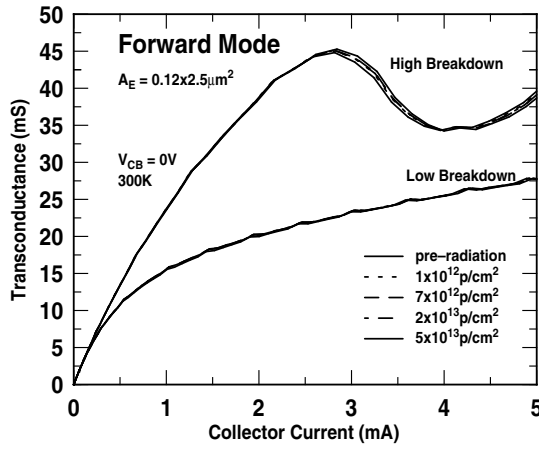


Fig. 10. Extrinsic transconductance for the high- and low-breakdown devices (4th-generation).

sic transconductance (g_m) of both high- and low-breakdown devices is shown in Figure 10. The onset of HBE clearly occurs at a much lower I_C than that of the low-breakdown device, a consequence of the lower N_C doping level in the high-breakdown device and in both cases, is insensitive to proton radiation, clearly good news from a circuit perspective.

Measurements to assess the impact of irradiation on neutral base recombination (NBR) is shown in Figure 11 for $V_{BE} = 0.66V$. It is evident that the low-breakdown device, with its increased N_C , exhibits a much stronger post-radiation NBR component at low V_{CB} , as manifested by the increased $I_B(V_{CB})/I_B(0)$ factor. This is the result of increased recombination of minority and majority carriers in the base. Increased base-recombination results in an increase in I_B and reduction in β as observed in Figure 6. In the case of the high-breakdown device, the post radiation NBR component is significantly less.

Figure 11 also demonstrates that the breakdown voltage, BV_{CEO} (extracted as the voltage at which $I_B(V_{CB})/I_B(0) = 0$) increases with fluence in the case of the high-breakdown device, but decreases in the case of the low-breakdown device. The low injection, forced- I_B output characteristics depicted in Figure 12 provide additional evidence of this result. The post-radiation output characteristics of the low-breakdown device demonstrates increased avalanche multiplication, and a reduced V_A , BV_{CEO} ,

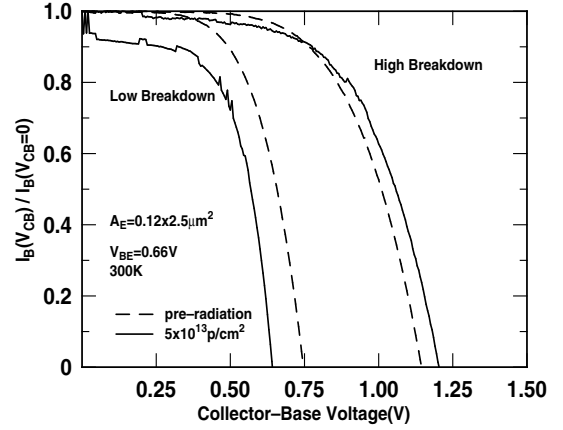


Fig. 11. Neutral base recombination for the high- and low-breakdown devices (4th-generation).

and β , whereas the results for the high-breakdown device indicate that these effects are not nearly as pronounced, and BV_{CEO} even *increases*. These results indicate again that strong electric

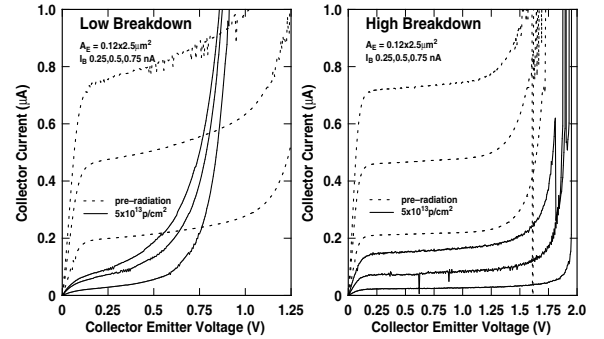


Fig. 12. Forced I_B output characteristics for high- and low-breakdown devices(4th-generation).

fields (as reported in [5]), this time in the CB junction (on account of high N_C), negatively impact the post-radiation device performance characteristics.

V. ac RESULTS

The transistor scattering parameters (S-parameters) for the low-breakdown device ($f_T = 350GHz$), were characterized to 45 GHz over a range of bias currents, each at a constant V_{CB} . This data was then subsequently de-embedded using standard "open-short" structures to calculate the small-signal current gain (h_{21}) and the Mason's unilateral gain (U). f_T data points were then obtained using a -20dB/decade slope extrapolation of h_{21} for different proton fluences, as shown in Figure 13 for both pre-radiation and a post-radiation fluence of 5×10^{13} p/cm². As evidenced in the figure, both pre- and post-radiation h_{21} data are remarkably robust. An overlay of pre- and post-radiation measurements of f_T vs J_C for 1st-, 2nd-, 3rd- and 4th-generation SiGe HBTs, shown in Figure 15 verify that their *ac* performance continues to be remarkably resistant to damage by ionizing radiation, even for novel device structures employing both aggressive vertical scaling and reduced thermal cycle processing. This is clearly excellent news. Specifically, in the case of the 4th-generation

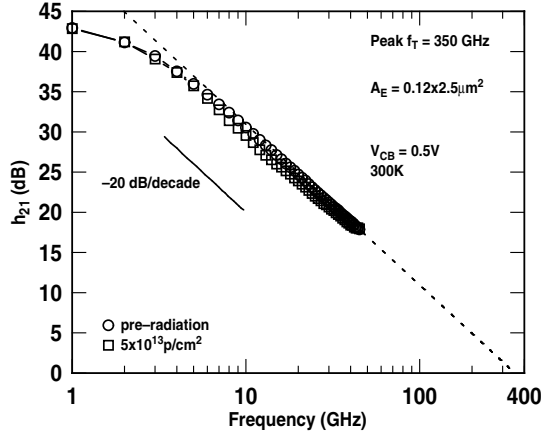


Fig. 13. h_{21} extrapolation for 4th-generation SiGe HBTs..

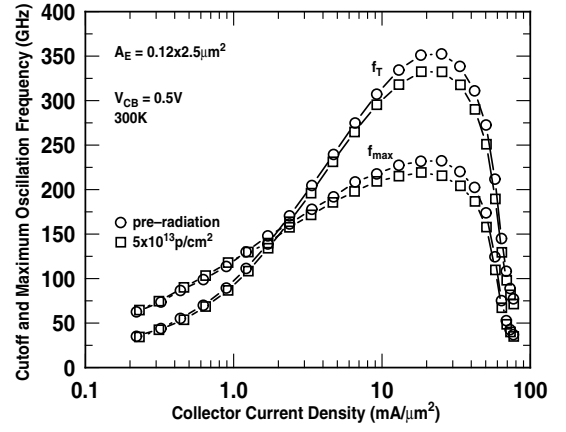


Fig. 15. Pre- and post-radiation f_T and f_{max} for 4th-generation SiGe HBTs.

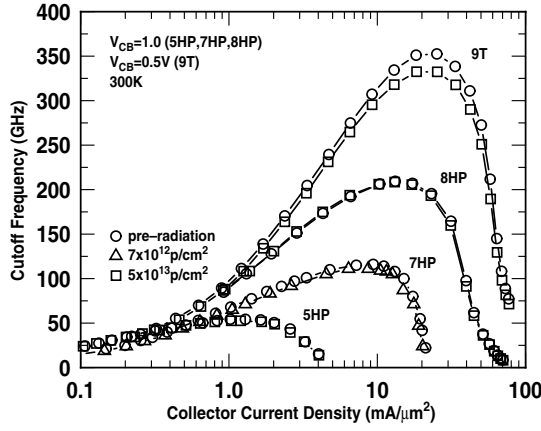


Fig. 14. Pre- and post-radiation f_T for 1st-, 2nd-, 3rd- and 4th-generation SiGe HBTs.

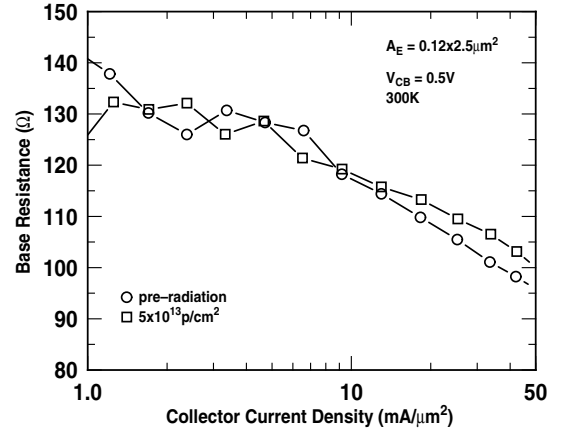


Fig. 16. Pre- and post-radiation r_{bb} variation with J_C (4th-generation SiGe HBTs).

SiGe HBT there is a moderate 6% decrease in both f_T and f_{max} as depicted in Figure 15.

The dynamic base resistance (r_{bb}), was extracted from measured S-parameters and is shown in Figure 16. A slight increase in r_{bb} at 5×10^{13} p/cm², for J_C close to peak f_T is observed and is consistent with the moderate 6% decrease in the peak f_{max} , previously attributed to displacement effects in the neutral base region and the deactivation of boron dopants [8]. For lower J_C values, pre- and post-radiation r_{bb} are both exhibit significant fluctuation. This can be attributed to the fact that small-signal parameter extraction in this lower bias regime may be less accurate on account of the smaller dynamic range of the VNA. Finally, the forward transit time (τ_{EC}), as a function of proton fluence, for 2nd-, 3rd- and 4th-generation SiGe HBTs are given in Figure 17. The vertical scaling methodologies outlined in [2] enables further reduction in τ_{EC} to a record value of 0.45 psec, as shown in the Figure. More importantly, τ_{EC} remains remarkably independent of proton fluence up to an extreme level of 1×10^{14} p/cm² in the case of the 3rd- and 4th-generation SiGe HBT-generation device. This is in stark contrast to the monotonically increasing relationship between τ_{EC} and fluence for the 2nd generation device, an indication that the new raised extrinsic base structure also affords carrier transit paths that are further removed from areas of high radiation induced trap density.

VI. SUMMARY

The proton tolerance of 4th-generation SiGe HBTs is assessed through critical analysis of the post-radiation effect on *ac* and *dc* figures-of-merit. Specifically a moderate 6% decrease is observed for both f_T and f_{max} (well within the measurement error of the setup) and β at peak f_T experiences less than 0.3% reduction. Both forward and inverse I_B leakage for the 3rd- and 4th-generation devices are significantly lower than that of previous technology nodes, a testament to inherent resilience of the raised extrinsic base structure in improving the isolation of the EB and CB junctions from radiation induced traps. Additionally, subtle differences in the response of 4th-generation devices with different collector doping have been explored. These results clearly indicate that SiGe HBTs continue to maintain excellent total dose tolerance in the midst of aggressive technology scaling yielding unprecedented device performance.

VII. ACKNOWLEDGEMENT

The authors would like to thank L. Cohn, K. LaBel, J. Lee, S. Nuttnick, G. Niu, A. Joseph, D. Harame, D. Herman, B. Meyerson, and the IBM SiGe team for their contributions.

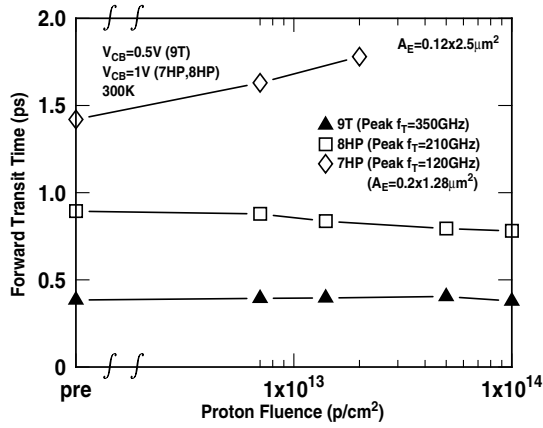


Fig. 17. The τ_{EC} variation with fluence for 2nd-, 3rd- and 4th-generation SiGe HBTs.

REFERENCES

- [1] J.D. Cressler and G. Niu, *Silicon-Germanium Heterojunction Bipolar Transistors*, Artech House, Boston, 2003.
- [2] J.-S. Rieh, B. Jagannathan, H. Chen, K.T. Schonenberg, D. Angell, A. Chinthakindi, J. Florkey, F. Golan, D. Greenberg, S. -J. Jeng, M. Khater, F. Pagette, C. Schnabel, P. Smith, A. Stricker, K. Vaed, R. Volant, D. Ahlgren, G. Freeman, K. Stein, and S. Subbanna, "SiGe HBTs with Cut-off Frequency of 350GHz," in *Technical Digest IEEE International Electron Devices Meeting*, pp. 771-774, 2002.
- [3] J.-S. Rieh, D. Greenberg, M. Khater, K.T. Schonenberg, S. -J. Jeng, F. Pagette, T. Adam, A. Chinthakindi, J. Florkey, B. Jagannathan, J. Johnson, R. Krishnasamy, D. Sanderson, C. Schnabel, P. Smith, A. Stricker, S. Sweeney, K. Vaed, T. Yanagisawa, D. Ahlgren, K. Stein, and G. Freeman, "SiGe HBTs for Millimeter-Wave Applications with Simultaneously Optimized f_T and f_{max} of 300GHz" in *Technical Digest IEEE Radio Frequency Integrated Circuits Symposium*, pp. 395-398, 2004.
- [4] E. O. Johnson, "Physical limitations on frequency and power parameters of transistors," *RCA Review*, vol. 26, pp. 163-177, 1965.
- [5] J.D. Cressler, M.C. Hamilton, G.S. Mullinax, Y. Li, G. Niu, C.J. Marshall, P.W. Marshall, H.S. Kim, M.J. Palmer, A.J. Joseph, and G. Freeman, "The Effects of proton Irradiation on the Lateral and Vertical Scaling of UHV/CVD SiGe HBT BiCMOS Technology," *IEEE Transactions on Nuclear Science*, vol. 47, pp. 2515-2520, Dec 2000.
- [6] B. Jagannathan, M. Khater, F. Pagette, J.-S. Rieh, D. Angell, H. Chen, J. Florkey, F. Golan, D. R. Greenberg, R. Groves, S. J. Jeng, J. Johnson, E. Mengistu, K.T. Schonenberg, C.M. Schnabel, P. Smith, A. Stricker, D. Ahlgren, G. Freeman, K. Stein, and S. Subbanna, "Self-Aligned SiGe NPN Transistors With 285 GHz f_{max} and 207 GHz f_T in a Manufacturable Technology," *IEEE Electron Device Letters*, vol. 23, pp. 258-260, May 2002.
- [7] J.D. Cressler, R. Krithivasan, G. Zhang, G. Niu, P.W. Marshall, H.S. Kim, R.A. Reed, M.J. Palmer, and A.J. Joseph, "An investigation of the origins of the variable proton tolerance in multiple SiGe HBT BiCMOS technology generations," *IEEE Transactions on Nuclear Science*, vol. 49, pp. 3203-3207, 2002.
- [8] Y. Lu, J.D. Cressler, R. Krithivasan, Y. Li, R.A. Reed, P.W. Marshall, C. Polar, G. Freeman, and D. Ahlgren, "Proton Tolerance of a Third Generation, 0.12µm 185 GHz SiGe HBT Technology," *IEEE Transactions on Nuclear Science*, vol. 50, pp. 1811-1815, Dec 2003.
- [9] K.M. Murray, W.J. Stapor, and C. Casteneda, "Calibrated charged particle radiation system with precision dosimetric measurement and control," *Nuclear Instruments and Methods in Physics Research*, vol. A281, pp.616-621, Sept 1989.
- [10] P.W. Marshall, C.J. Dale, M.A. Carts, and K.A. Label, "Particle-induced bit errors in high performance fiber optic data links for satellite data management," *IEEE Transactions on Nuclear Science*, vol. 41, pp. 1958-1965, Dec 1994.
- [11] S.Zhang, G. Niu, J.D. Cressler, S.D. Clark, and D.C. Ahlgren, "The effects of proton irradiation on the RF performance of SiGe HBTs," *IEEE Transactions on Nuclear Science*, vol. 46, pp. 1716-1721, 1999.
- [12] C.T. Kirk "Theory of transistor cutoff frequency falloff at high current densities" *IRE Transactions on Electron Devices*, vol. 3, pp. 164-170, 1964.
- [13] B.G. Malm, T. Johansson, T. Arnborg, H. Norstrom, J.V. Grahn, M. Ostling, "Implanted collector profile optimization in a SiGe HBT process," *Solid State Electronics*, vol. 45, pp. 399-404, March 2001.
- [14] A.J. Joseph, J.D. Cressler, D.M. Richey, G. Niu "Optimization of SiGe HBTs for operation at high current densities," *IEEE Transactions on Electron Devices*, vol. 46, pp. 1347-1354, July 1999.